Anatomical origin and computational role of diversity in the response properties of cortical neurons*

Kalanit Grill Spector† Shimon Edelman† Rafael Malach‡
Departments of †Applied Mathematics and Computer Science and ‡Neurobiology
The Weizmann Institute of Science
Rehovot 76100, Israel
{kalanit,edelman}@wisdom.weizmann.ac.il bnmalach@weizmann.weizmann.ac.il

Abstract

The maximization of diversity of neuronal response properties has been recently suggested as an organizing principle for the formation of such prominent features of the functional architecture of the brain as the cortical columns and the associated patchy projection patterns (Malach, 1994). We report a computational study of two aspects of this hypothesis. First, we show that maximal diversity is attained when the ratio of dendritic and axonal arbor sizes is equal to one, as it has been found in many cortical areas and across species (Lund et al., 1993; Malach, 1994). Second, we show that maximization of diversity leads to better performance in two case studies: in systems of receptive fields implementing steerable/shiftable filters, and in matching spatially distributed signals, a problem that arises in visual tasks such as stereopsis, motion processing, and recognition.

1 Introduction

A fundamental feature of cortical architecture is its columnar organization, manifested in the tendency of neurons with similar properties to be organized in columns that run perpendicular to the cortical surface. This organization of the cortex was initially discovered by physiological experiments (Mountcastle, 1957; Hubel and Wiesel, 1962), and subsequently confirmed with the demonstration of histologically defined columns. Tracing experiments have shown that axonal projections throughout the cerebral cortex tend to be organized in vertically aligned clusters or patches. In particular, intrinsic horizontal connections linking neighboring cortical sites, which may extend up to $2-3$ mm, have a striking tendency to arborize selectively in preferred sites, forming distinct axonal patches $200-300$ μm in diameter.

Recently, it has been observed (Malach, 1992; Amir et al., 1993; Malach et al., 1993) that the size of these patches matches closely the average diameter of individual dendritic arbors of upper-layer pyramidal cells. Insofar as this correlation between column or patch size and dendritic spread is a fundamental property that holds throughout various cortical areas and across species (Lund et al., 1993), one is led to assume that it constitutes an important characteristic of the columnar architecture of the cortex. Determining its functional significance may, therefore, shed light on the principles that drive the evolution of the cortical architecture.

One such driving principle may be the maximization of diversity in the neuronal population in the cortex (Malach, 1994). According to this hypothesis, matching the sizes of the axonal patches and the dendritic arbors causes neighboring neurons to develop slightly different functional selectivity profiles, resulting in an even spread of response preferences across the cortical population, and in an improvement of the brain's ability to process the variety of stimuli likely to be encountered by the owner of the brain in the environment.

The present work concentrates on two aspects of this hypothesis. First, we address the basic question of the manner whereby the patchy columnar architecture can support the maximization of diversity. In section 2, we

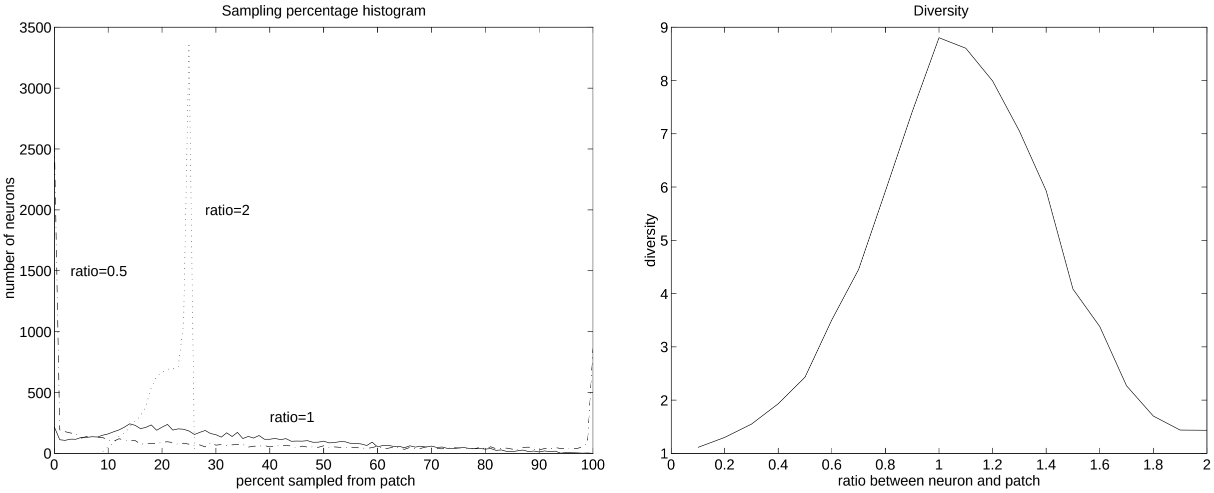

Figure 1: *Left:* histograms of the percentage of patch-originated input to the neurons, plotted for three values of the ratio r between the dendritic arbor and the patch diameter (0.5, 1.0, 2.0). The flattest histogram is obtained for $r = 1.0$ *Right:* the diversity of neuronal properties (as defined in section 2) vs. r. The maximum is attained for $r = 1.0$, a value compatible with the anatomical data.

propose a quantitative definition of diversity and analyze its dependence on the ratio of axonal and dendritic patch sizes, showing that a maximum is attained when that ratio is equal to 1. Second, we explore the possible computational rationale behind the maximization of diversity. In section 3, we show that diversity in orientation and location of receptive fields (RFs) is beneficial when considered in the framework of steerable/shiftable filter generation. In section 4, we consider the influence of diversity in RF location on the ability of RF-based systems to match spatially distributed signals – a problem that arises in visual tasks such as stereopsis, motion processing, and recognition.

2 An anatomical correlate of neuronal sampling diversity

To test the effect of the ratio between axonal patch and dendritic arbor size on the diversity of the neuronal population, we conducted computer simulations based on anatomical data concerning patchy projections (Rockland and Lund, 1982; Lund et al., 1993; Malach, 1992; Malach et al., 1993).[1] The patches were modeled by disks, placed at regular intervals of twice the patch diameter, as revealed by anatomical labeling. Dendritic arbors were also modeled by disks, whose radii were manipulated in different simulations. The arbors were placed randomly over the axonal patches, at a density of $10,000$ neurons per patch. We then calculated the amount of patch-related information sampled by each neuron, defined to be proportional to the area of overlap of the dendritic tree and the patch. The results of the calculations for three values of the ratio of patch and arbor diameters appear in Figure 1.

The presence of two peaks in the histogram obtained with the arbor/patch ratio $r = 0.5$ indicates that two dominant groups are formed in the population, the first receiving most of its input from the patch, and the second – from the inter-patch sources. A value of $r = 2.0$, for which the dendritic arbors are larger than the axonal patch size, yields near uniformity of sampling properties, with most of the neurons receiving mostly patch-originated input, as apparent from the single large peak in the histogram.

[*]**Category:** Neuroscience; **Keywords:** functional architecture, orientation columns, steerable filters, matching, diversity; **Presentation preference:** oral.

[1]Necessary conditions for obtaining dendritic sampling diversity are that dendritic arbors cross freely through column borders, and that dendrites which cross column borders sample with equal probability from patch and inter-patch compartments. These assumptions were shown to be valid in (Malach, 1992; Malach, 1994).

To quantify the notion of diversity, we defined it as:

$$diversity \sim \frac{1}{< |\frac{dn}{dp}| >} \tag{1}$$

where $n(p)$ is the number of neurons that receive p percent of their inputs from the patch, and $< \cdot >$ denotes average over all values of p. Figure 1, right, shows that diversity is maximized when the size of the dendritic arbors matches that of the axonal patches, in accordance with the anatomical data. This result confirms the diversity maximization hypothesis stated in (Malach, 1994).

3 Orientation tuning as a functional manifestation of neuronal sampling diversity

In this section, we consider the smooth gradation of orientation tuning across the cortical surface in area V1 in mammals as a possible consequence of highly diverse sampling in the underlying neuronal population. We start with some background regarding the orientation columns in V1.

3.1 Background

The orientation columns in V1 are perhaps the best-known example of functional architecture found in the cortex. On the basis of single unit recordings (Hubel and Wiesel, 1962) reported that cells encountered in penetrations perpendicular to the cortical surface have similar orientation selectivity. In tangential penetrations, orientation preference shifts as the electrode advances. In their early recordings, Hubel and Wiesel reported discrete shifts rather than a continuous change in orientation preference. In subsequent recordings they found that orientation shifts can vary more smoothly, and concluded that orientation preference varies continuously throughout V1 (Hubel and Wiesel, 1977). Cortical maps obtained by optical imaging (Grinvald et al., 1986) reveal that orientation columns are patchy rather then slab-like, i.e., domains corresponding to a single orientation appear as a mosaic of round patches, which tend to form pinwheel-like structures. Moreover, incremental changes in the orientation of the stimulus were found to lead to smooth shifts in the positions of these domains. We hypothesize that this smooth variation in orientation selectivity found in V1 originates in patchy projections, combined with diversity in the sampling properties of cortical neurons sampling from these projections. The simulations described in the rest of this section substantiate this hypothesis.

3.2 Modeling orientation columns: computer simulations

The goal of the simulations was to demonstrate that a limited number of discretely tuned elements can give rise to a continuum of responses. To set the size of the original discrete orientation columns, we invoked the notion of a point image (MacIlwain, 1976; MacIlwain, 1986), defined as the minimal cortical separation of cells with non-overlapping RFs. Thus, we created a network of orientation columns, whose size was determined by the diameter of their constituent RFs. Each column was tuned to a specific angle, and located at an approximately constant distance from another column with the same orientation tuning (we allowed some scatter in the location of the RFs). The RFs of adjacent units with the same orientation preference were overlapping, and the amount of overlap was determined by the number of RFs incorporated into the network. The preferred orientations were equally spaced at angles between 0 and π. The RFs used in the simulations were modeled by a product of a 2D Gaussian G_1, with center at $\vec{r_j}$, and an orientation selective filter G_2, with optimal angle θ_i: $G(\vec{r}, \vec{r_j}, \theta, \theta_i) = G_1(\vec{r}, \vec{r_j})G_2(\theta, \theta_i)$

According to the recent results on shiftable/steerable filters (Freeman and Adelson, 1991; Simoncelli et al., 1992), a RF located at $\vec{r_0}$ and tuned to the orientation ϕ_0 can be obtained by a linear combination of basis RFs, as follows:

$$G(\vec{r}, \vec{r_0}, \theta, \phi_0) = \textstyle\sum_{j=0}^{M-1} \sum_{i=0}^{N-1} b_j(\vec{r_0})k_i(\phi_0)G(\vec{r}, \vec{r_j}, \theta, \theta_i) \tag{2}$$

$$= \textstyle\sum_{j=0}^{M-1} b_j(\vec{r_0})G_1(\vec{r}, \vec{r_j}) \sum_{i=0}^{N-1} k_i(\phi_0)G_2(\theta, \theta_i) \tag{3}$$

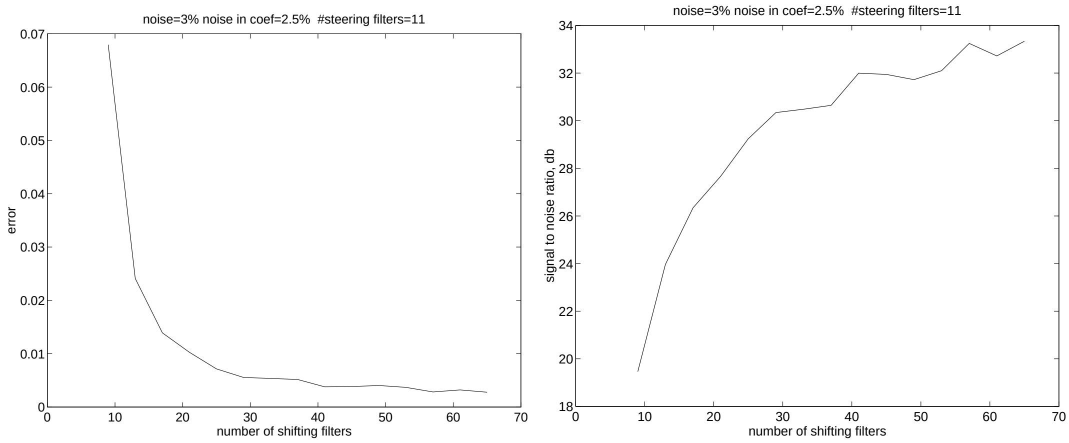

Figure 2: The effects of (independent) noise in the basis RFs and in the steering/shifting coefficients. *Left:* the approximation error vs. the number of basis RFs used in the linear combination. *Right:* the signal to noise ratio vs. the number of basis RFs. The SNR values were calculated as $10\log_{10}(signal\ energy/noise\ energy)$. Adding RFs to the basis increases the accuracy of the resultant interpolated RF.

From equation 3 it is clear that the linear combination is equivalent to an outer-product of the shifted RF and the steered RF. The numbers $\{k_i(\phi_0)\}_{i=0}^{N-1}$ and $\{b_j(\vec{r_0})\}_{j=0}^{M-1}$ denote the steering and shifting coefficients, respectively. Since orientation and localization are independent parameters, the steering coefficients can be calculated separately from the shifting coefficients. The number of steering coefficients depends on the polar Fourier bandwidth of the basis RF, while the number of steering filters is inversely proportional to the basis RF size. Our simulations show that in the presence of noise this minimal basis has to be extended (see Figure 2).

The results of running this simulation for several RF sizes are shown in Figure 3, left. As predicted by the mathematical formulation, the number of basis RFs required to approximate a desired RF is inversely proportional to the size of the basis RFs. The right panel in Figure 3 shows that as the basis RFs are made bigger, fewer of them are needed to achieve a given approximation error.

3.3 Steerability and biological considerations

The anatomical finding that the columnar "borders" are freely crossed by dendritic and axonal arbors (Malach, 1992), and the mathematical properties of shiftable/steerable filters outlined above suggest that the columnar architecture in V1 provides a basis for creating a continuum of RF properties, rather that being a form of organizing RFs in discrete bins. Computationally, this may be possible if the input to neurons is a linear combination of outputs of several RFs, as in equation 3. Is this assumption warranted by other anatomical and physiological data regarding cortical interconnection patterns?

Horseradish peroxidase (HRP) labeling studies (Rockland and Lund, 1982) have shown that lateral connections of orientation columns extend to a range of $2-4\ mm$. In other studies that used 2DG autoradiography and retrograde labeling, connectivity patterns were superimposed on functional maps (Gilbert and Wiesel, 1989). The results showed that cells tended to connect to cells of like orientation preference. The relationship between functionally defined columns and patchy connections was studied by (Malach et al., 1993). They used optical imaging techniques to construct functional maps of orientation columns, then targeted injections of biocytin tracer to selected functional domains. Their results show that long-range connections, extending one mm or more, tend to link cells with like orientation preference. In the short range, up to 400 μm from the injection site, connections were made to cells of diverse orientation preferences. The selectivity of the short-range connections is markedly disrupted probably because dendritic arbors and axonal connections freely cross orientation column borders.

We suggest that the long-range connections, which connect cells of like orientation preference, provide the inputs necessary to shift the position of the desired RF, while the short-range connections, which connect cells

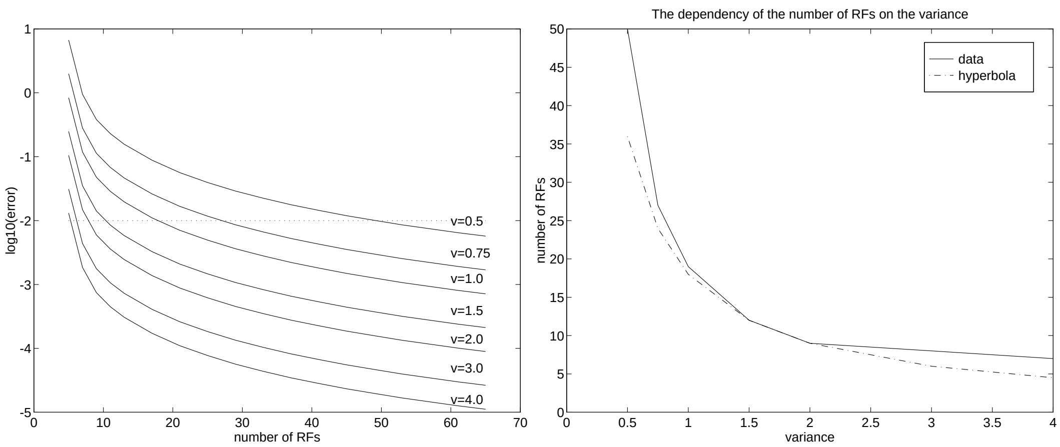

Figure 3: *Left:* error of the steering/shifting approximation for several basis RF sizes. *Right:* the number of basis RFs required to achieve a given error for different sizes of the basis RFs. The dashed line is a hyperbola $num\ RFs \times size = const.$

of diverse orientation preference, provide the connections needed to steer the RF to an arbitrary angle.[2]

4 Matching with patchy connections

4.1 The problem of matching

Many visual tasks require matching between images taken at different points in space (as in binocular stereopsis) or time (as in motion processing). The first and foremost problem faced by a biological system in solving these tasks is that the images to be compared are not represented as such anywhere in the system: instead of images, there are patterns of activities of RFs, whose profile parameters and location in the visual field are, to a considerable extent, random.

It is now a matter of common agreement that while the cortex is not wired as precisely as an electronic device, neither it is a free-for-all jumble of connections completely devoid of order. On the one hand, the intrinsic patchy connections exhibit a certain degree of wiring precision. On the other hand, there is also a significant patch-interpatch mixing (Malach, 1992), and a typical patch has a non-negligible diameter of $200 - 300\ \mu m$. The number of axonal arborizations in a patch is of an order of magnitude of 10^4, and about the same number of dendrites sample it. On the average each dendritic tree makes one synapse with an overlapping axonal arbor (Braitenberg and Schuz, 1991; Schuz, 1992), but the degree of target specificity in a patch is difficult to estimate. An additional complication is due to the plasticity of cortical connections, as evident both in the classical deprivation experiments (Hubel, 1988), and also in the data on behaviorally controlled stimulation (Merzenich et al., 1990; Recanzone et al., 1992). (LeVay, 1989) suggests that intrinsic patchy connections could arise during development in response to a rule of the kind "cells that fire together wire together". It is possible that these connections emerge from profuse non-patchy projections, by a selective activity-dependent elimination of synapses.

Patchy connections are not, however, necessarily bad news. As we show in the following section, a system composed of scattered RFs with smooth and overlapping tuning functions can perform matching precisely by allowing patchy connections between domains. Moreover, the weights that must be given to the various inputs that feed a RF carrying out the match are identical to the coefficients that would be generated by a learning algorithm required to capture a certain well-defined input-output relationship from pairs of examples.

[2]Our simulations also support the findings of (Dow et al., 1981) on the relationship between cortical magnification and RF size. They reported that foveal RFs, of size $25' - 30'$, show more overlap than peripheral, of size about $2° - 4°$, in accordance to our results, as depicted in Figure 3.

4.2 Matching patchy signals: a mathematical formulation

We formulate the matching problem according to the scheme sketched in Figure 4, in which the dendrites of unit C sample two domains, A and B. The dendritic arbor is a patch of diameter equal to that of the projection profile of cells feeding areas A and B. This profile is modeled by a multi-dimensional Gaussian. The task faced by unit C is to determine the degree to which the activity patterns in domains A and B match.

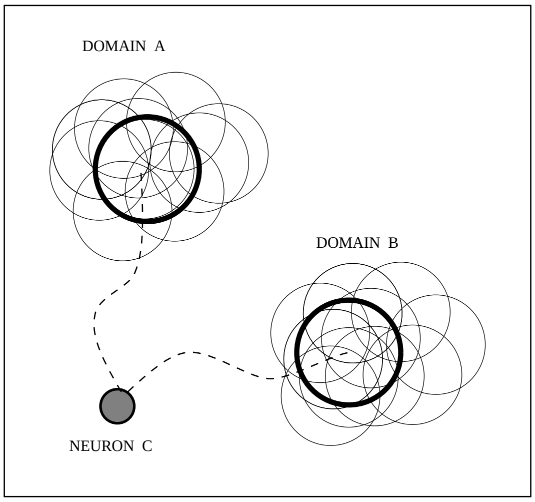

Figure 4: Unit C receives patchy input from areas A and B which contain receptors with overlapping RFs.

Let ϕ_{jp} and θ_{jp} be the responses of the j'th unit in domains A and B, respectively, to an input $\vec{x_p}$:

$$\phi_{jp}, \theta_{jp} = \exp\{\frac{-(\vec{x_p} - \vec{x_j})^2}{2\sigma^2}\} \tag{4}$$

where $\vec{x_j}$ be the optimal pattern to which the j'th unit is tuned. If, for example, domains A and B contain orientation selective cells, then $\vec{x_j}$ would be the optimal combination of orientation and location of a bar stimulus. For simplicity we assume that all the RFs are of the same size σ, that unit C samples the same number of neurons N from both domains, and that the input from each domain to unit C is a linear combination of the responses of the units in each area. The input to C from domain A, with $\vec{x_p}$ presented to the system is then:

$$A_{in} = \sum_{j=1}^{N} a_j \phi_{jp} \tag{5}$$

The problem is to find coefficients $\{a_j\}$ and $\{b_j\}$ such that on a given set of inputs $\{\vec{x_p}\}$ the outputs of domains A and B will match. We define the matching error as follows:

$$E_m = \sum_{p=1}^{P} \left(\sum_{i=1}^{N} a_i \phi_{ip} - \sum_{i=1}^{N} b_i \theta_{ip} \right)^2 \tag{6}$$

Theorem 1 *The desired matching coefficients can be generated by an algorithm trained to learn an input/output mapping from a set of examples.*

As an example of the learning algorithm, one may chose radial basis function (RBF) approximation (Poggio and Girosi, 1990). This approach is particularly suitable for our purpose, because the basis functions in RBF approximation can be regarded as multidimensional Gaussian RFs.

Proof: To find the coefficients we differentiate equation 6 with respect to each coefficient, The following linear system is obtained:

$$\frac{\partial E_m}{\partial a_j} = 0 \Rightarrow \quad \sum_{p=1}^{P} \phi_{jp} \sum_{k=1}^{N} a_k \phi_{kp} = \sum_{p=1}^{P} \phi_{jp} \sum_{k=1}^{N} b_k \theta_{kp} \qquad \forall j = 1...N \tag{7}$$

The inner sums in equation 7 are the outputs of the two domains on the training set (cf. equation 5), and we require that they match, for each example in the training set. Therefore, to calculate the coefficients, the following set of equations must be solved for $\{a_j\}$ and $\{b_j\}$:

$$\sum_{k=1}^{N} a_k \phi_{kp} = \sum_{k=1}^{N} b_k \theta_{kp} = t_p \qquad \forall p = 1...P \tag{8}$$

where t_p is the required output for the p'th example. Consider now an algorithm that learns an input-output relation by minimizing the total error on a given training set:

$$E = \sum_{p=1}^{P} \left(\sum_{i=1}^{N} a_i \phi_{ip} - t_p \right)^2 \tag{9}$$

Minimizing the error in equation 9 yields the same system for a_i and b_i as equation 8. $\Box$

Further research is needed to generalize this result to the case when the two inputs should be related by a function which is not the identity. For example, in bilateral symmetry detection the patterns in A and B should be, in a sense, mirror images of each other. In general, therefore, to find the synaptic weights for unit C, one must minimize:

$$E_m = \sum_{p=1}^{P} \left(\sum_{i=1}^{N} a_i \phi_{ip} - f\left(\sum_{i=1}^{N} b_i \theta_{ip} \right) \right)^2 \tag{10}$$

5 Summary

Our results show that maximal diversity of neuronal response properties is attained when the ratio of dendritic and axonal arbor sizes is equal to 1, a value found in many cortical areas and across species (Lund et al., 1993). It also appears that maximization of diversity leads to better performance in systems of receptive fields implementing steerable/shiftable filters, which may be necessary for generating the seemingly continuous range of orientation selectivity found in V1, and in matching spatially distributed signals. Thus, the maximization of diversity of neuronal response properties considered as a cortical organization principle (Malach, 1994) may have the double advantage of accounting for the formation of the cortical columns and the associated patchy projection patterns, and of explaining how systems of receptive fields can support functions such as the generation of precise response tuning from imprecise distributed inputs, and the matching of distributed signals, a problem that arises in visual tasks such as stereopsis, motion processing, and recognition.

References

Amir, Y., Harel, M., and Malach, R. (1993). Cortical hierarchy reflected in the organization of intrinsic connections in macaque monkey visual cortex. *J. Comp. Neurobiol.*, 334:19–46.

Braitenberg, V. and Schuz, A. (1991). *Anatomy of the cortex, statistics and geometry.* Springer, Berlin, Heidelberg, New-York.

Dow, B., Cynader, A., Vautin, R., and Bauer, R. (1981). Magnification factor and receptive field size in foveal striate cortex of the monkey. *Experimental Brain Research*, 44:213–228.

Freeman, W. and Adelson, E. (1991). The design and use of steerable filters. *IEEE Transactions on Pattern Analysis and Machine Intelligence*, 13:891–906.

Gilbert, C. and Wiesel, T. (1989). Columnar specificity of intrinsic horizontal and corticocortical connections in cat visual cortex. *Journal of Neuroscience*, 9:2432–2442.

Grinvald, A., Lieke, T., Gilbert, R. F. C., and Wiesel, T. (1986). Functional architecture of the cortex as revealed by optical imaging of intrinsic signals. *Nature*, 324:361–364.

Hubel, D. (1988). *Eye, Brain,and Vision.* Scientific American Library.

Hubel, D. and Wiesel, T. (1962). Binocular interactions and functional architecture in the cat's visual cortex. *Journal of Physiology*, 160:106–154.

Hubel, D. and Wiesel, T. (1977). Functional architecture of macaque monkey visual cortex. *Proceedings of the Royal Society of London B*, 198:1–59.

LeVay, S. (1989). The patchy intrinsic projections of the visual cortex. *Progress in Brain Research*, 75:247–261.

Lund, J. S., Yoshita, S., and Levitt, J. B. (1993). Comparison of intrinsic connections in different areas of macaque cerebral cortex. *Cerebral Cortex*, 3:148–162.

MacIlwain, J. (1976). Large receptive fields and spatial transformations in the visual system. *International Review Physiology*, 10:223–248.

MacIlwain, J. (1986). Point images in the visual system: new interest in an old idea. *Trends in Neurosciences*, 9:354–358.

Malach, R. (1992). Dendritic sampling across processing streams in monkey striate cortex. *Journal of Comparative Neurobiology*, 315:305–312.

Malach, R. (1994). Cortical columns as devices for maximizing neuronal diversity. *Trends in Neurosciences*, 17:101–104.

Malach, R., Amir, Y., Harel, M., and Grinvald, A. (1993). Relationship between intrinsic connections and functional architecture,revealed by optical imaging and in vivo targeted biocytin injections in primate striate cortex. *Proceedings of the National Academy of Science, USA*, 90:10469–10473.

Merzenich, M., Jenkins, W., Ochs, M., Allard, M., and Guic-Robles, E. (1990). Functional reorganization of primary somatosensory cortex in adult owl monkeys after behaviorally controlled tactile stimulation. *Journal of Neurophysiology*, 63:82–104.

Mountcastle, V. B. (1957). Modality and topographic properties of single neurons of cat's somatic sensory cortex. *Journal of Neurophysiology*, 20:408–434.

Poggio, T. and Girosi, F. (1990). Regularization algorithms for learning that are equivalent to multilayer networks. *Science*, 247:978–982.

Recanzone, G., Merzenich, M., Jenkins, W., Grajski, K., and Dinse, H. (1992). Topographic reorganization of the hand representation in cortical area 3b of owl monkeys trained in a frequency discrimination task. *Journal of Neurophysiology*, 67:1031–1056.

Rockland, K. and Lund, J. (1982). Widespread periodic intrinsic connections in the tree shrew visual cortex. *Science*, 215:1532–1534.

Schuz, A. (1992). Randomness and constraints in the cortical neuropil. In Aertsen, A. and Braitenberg, V., editors, *Information processing in the cortex*, pages 3–19. Springer-Verlag, Berlin Heidelberg New York.

Simoncelli, E., Freeman, W., Adelson, E., and Heeger, D. (1992). Shiftable multiscale transformations. *IEEE Transactions on Information Theory*, 38:587–607.